Journal of Archaeological Science: Reports 36 (2021) 102814

Contents lists available at ScienceDirect

Journal of Archaeological Science: Reports

journal homepage: www.elsevier.com/locate/jasrep

Methods for determination of the source of iron in precontact Inuit and Dorset culture artifacts from the Canadian Arctic

Matthew J.O. Svensson [a], Stephen A. Kissin [a,*], Marie-Claude Corbeil [b], Peter Whitridge [c], James W. Helmer [d]

[a] Department of Geology, Lakehead University, Thunder Bay, Ontario P7B 5E1, Canada; Present address: Department of Earth Sciences/The Institute for Earth and Space Exploration, The University of Western Ontario, London, Ontario N6A 3K7, Canada
[b] Conservation Science Division, Canadian Conservation Institute, Department of Canadian Heritage, 1030 Innes Road, Ottawa, Ontario K1B 4S7, Canada
[c] Department of Archaeology, Memorial University of Newfoundland, St. John's, Newfoundland and Labrador A1C 5S7, Canada
[d] Department of Anthropology and Archeology, University of Calgary, 2500 University Drive NW, Calgary, Alberta T2N 1N4, Canada

ARTICLE INFO

Keywords:
Canadian Arctic
Dorset culture
Precontact Inuit
Norse
Meteorite
Iron

ABSTRACT

The period during which Dorset Culture peoples and precontact Inuit used iron was widespread and overlapped the appearance of the Norse in Greenland. In Greenland and Arctic Canada, three sources of iron in artifacts have been reported: terrestrial native iron, Norse wrought iron and meteoritic iron from the Cape York iron meteorite. We investigated the source of iron from fourteen samples of iron artifacts recovered from one precontact Inuit and three Dorset culture sites. Polished mm-scale samples mounted in polyester resin blocks yielding a roughly rectangular 1 × 2 mm cross section to preserve as much of each sample as possible were examined. Petrographic examinations by reflected light microscopy and SEM observation coupled with energy-dispersive analysis revealed the presence of Widmanstätten structure (an intergrowth of kamacite and taenite), a suite of minerals comprising kamacite, taenite, daubreelite and schreibersite and nickel-content at iron meteorite levels indicating all fourteen samples were unambiguously of meteoritic origin. With the meteoritic origin confirmed, Goldstein's (1965) model relating half-width of the kamacite lamellae in the Widmanstätten patterns to the Ni-content of the lamellae was used to determine whether the meteoritic iron originated from the Cape York meteorite. A test of the method used the mean kamacite bandwidth and the bulk Ni-content of the Cape York mass Savik I, which demonstrated the validity of the basis of the method. Using the experimentally-derived relation between kamacite half-width of the bands and composition of the kamacite, the nickel-content of the kamacite lamellae ranged from 6.13 to 6.61 wt% Ni. These compositions are consistent with bandwidths that are narrower than the mean for Cape York, the anticipated source. The discrepancy may be attributed to flattening of the kamacite lamellae by cold working in the manufacture of the artifacts. As well, it has been shown that a range of bandwidths is typical in large iron meteorites such as Cape York. Thus, this method cannot definitively identify Cape York as the source of the meteoritic iron in the fourteen samples; however, the results can serve to identify meteoritic artifacts if the material that has not been intensively cold worked and if sufficient bandwidths can be measured in order to establish a mean thickness.

1. Introduction

The use of metal implements by native peoples was widespread in western Greenland (Buchwald, 1975); however, metal artifacts from archeological sites in Canada are less common. Early discoveries of metal artifacts are described by McCartney and Mack (1973), McCartney (1991) and references therein. Their work on artifacts from western Hudson Bay sites revealed the southernmost occurrences of iron artifacts known in Canada. Neutron activation analyses of two samples from McCartney and Mack's (1973) study yielded trace and minor element compositions consistent with that of the Cape York iron meteorite of the west Greenland coast. Petrographic examinations of their entire suite of artifacts revealed that most were of meteoritic origin with some of European origin.

McCartney and Kimberlin (1988) subsequently reported on a collection of 28 iron artifacts from two precontact Inuit sites on

* Corresponding author at: Department of Geology, Lakehead University, Thunder Bay, Ontario P7B 5E1, Canada.
E-mail address: sakissin@lakeheadu.ca (S.A. Kissin).

https://doi.org/10.1016/j.jasrep.2021.102814
Received 9 January 2020; Received in revised form 11 January 2021; Accepted 14 January 2021
Available online 15 March 2021
2352-409X/

Fig. 1. Typical iron artifacts analyzed in this study (QjJx-1 site). Scale in cm.

Somerset Island. Thirteen of the artifacts were analyzed for diagnostic trace and minor elements by neutron activation analysis. The compositions of ten were found to be consistent with the Cape York meteorite, whereas two were believed to be of Norse origin, and one was from an apparently unknown meteorite.

The present study deals with a suite of fourteen artifacts from Dorset Culture and precontact Inuit sites from the Canadian Arctic Archipelago. These iron artifacts are highly oxidized, and the source of the metal is obscure (Fig. 1). The Qariaraqyuk samples had been previously analyzed for nickel-content and tentatively determined to be of meteoritic origin (Corbeil, 1996b; Whitridge, 1999; 2002). The 10 specimens from Arvik and Tasiarulik had also been previously analyzed for nickel and had been identified as of meteoritic origin based on bulk Ni-content consistent with the Cape York meteorite (Corbeil, 1996a; Lemoine et al., 2003).

The highly oxidized state of the artifacts together with the wishes of the Canadian Conservation Institute, Department of Canadian Heritage, that the artifacts be preserved as much as possible dictated that identification of the source be determined utilizing as little of the artifacts as possible. In particular, this requirement and the condition of the specimens makes neutron activation analysis inapplicable. This problem was noted as well by Buchwald and Mosdal (1985) in their studies of Greenland artifacts. Three possible sources for the metal in Inuit artifacts were discussed by Buchwald (1975) and Buchwald and Mosdal (1985). As previously discussed, meteoritic iron was widely employed in west Greenland and has been recovered from archeological sites from the Canadian Arctic Archipelago and as far south as the western side of Hudson Bay (McCartney and Mack, 1973). The meteoritic iron has almost universally shown to derive from the Cape York meteorite (e.g., McCartney and Kimberlin, 1988).

As reviewed by Goldstein et al. (2009), three structural types of iron meteorites are known: hexahedrites, octahedrites and ataxites. Octahedrites are the most abundant type, so named as they consist of kamacite (α-Fe) lamellae separated by lamellae of taenite (γ-Fe) arranged parallel to the faces of an octahedron, producing the Widmanstätten structure. The bulk composition of octahedrites is 6–$\sim$12 wt% Ni and is inversely related to the width of the kamacite lamellae. Hexahedites contain 5–6.5 wt% Ni and are entirely composed of kamacite, thus do not possess the Widmanstätten structure. Ataxites contain $\sim$ 10 to $>$ 20 wt% Ni and do not possess the Widmanstätten structure, although they do possess an oriented microstructure.

The only known iron meteorite from the Canadian Arctic and Greenland is the Cape York (Greenland) octahedrite (Buchwald, 1975). Although meteoritic iron artifacts have almost universally been shown to derive from the Cape York meteorite (e.g. McCartney and Kimberlin, 1988), one specimen in their study was from a meteorite of unknown origin. Thus, it is possible that sources of meteoritic metal other than Cape York exist but are not known at present.

A second possible source of iron is of European origin ranging from Norse sources, which likely date from the Norse colonization of Greenland and possibly from Norse exploration of the Canadian Arctic, to later European exploration in the Arctic in the case of precontact Inuit sites. As discussed by McGovern (1979; 1980), Norse settlement in Greenland began at 985 CE. Population centers were in two areas known as the Eastern Settlement near the southern tip of Greenland and the Western Settlement farther north along the west coast of Greenland. Contact between the Norse and Inuit was known to occur, although the contact may have been hostile. The Western Settlement was found to have been deserted by ca. 1350, although the reason for the disappearance of the population is unknown. The Eastern Settlement existed until ca. 1450, when its population also mysteriously disappeared. The abandoned Norse settlements were exploited by the precontact Inuit until ca. 1620, when the arrival of Dutch and English whalers provided an alternative source for metal articles through trade.

The use of iron tools bears on the interaction between Dorset culture groups and precontact Inuit, and between precontact Inuit and the Norse settlers of Greenland. The Dorset pre-Inuit culture has its origins in Arctic Small Tool Tradition groups that colonized the North American Arctic from Siberia around 4500 BP (Raghavan et al., 2014; Wright, 1995). The pre-Inuit migrated eastward, rapidly occupying Arctic Canada and Greenland (Friesen, 2016; Wright, 1995). Later pre-Inuit groups are assigned archaeologically to the Dorset culture, which existed between ca. 500 BCE and perhaps 1300 CE, although there is currently much archaeological disagreement over the timing of the Dorset demise.

The precontact Inuit entered the eastern Arctic and Greenland from the west at a time originally believed to be ca. 1000 CE (e.g. Maxwell, 1985; Wright, 1995). More recent dating and some reinterpretation of earlier data currently indicates that the arrival of the Inuit probably occurred between the late twelfth and mid thirteenth centuries (Whitridge, 2016). Moreover, the expansion into the eastern Arctic was rapid, occurring within several generations rather than hundreds of years (McGhee, 2009).

The succession from Dorset culture to precontact Inuit has long been a matter of controversy (Appelt et al., 2016); there may have been a century or more of temporal overlap and occasional interaction or Late Dorset culture may have been essentially extinct by the time Inuit arrived in the eastern Arctic (Park, 2016). In either case, recent genetic studies indicate that the two groups are genetically unrelated (Raghavan et al., 2014). The precontact Inuit were in contact with the Norse in Greenland and likely in some areas in Canada. Precontact Inuit archeological sites sometimes contain abundant artifacts of meteoritic iron, Norse iron, and even some terrestrial iron (Buchwald, 2001; Buchwald and Mosdal, 1985). The interaction with the Norse has been discussed by a number of workers (Appelt and Gulløv, 2009; Schledermann, 1980; McGovern, 1979). Although interactions were not always peaceful (McGovern, 1980), trade for, or scavenging of, wrought iron may well have occurred.

McCartney and Mack (1973) stated that there was no contact between the Norse and Dorset groups based on their findings. This view prevailed for some time based on a perceived gap between the ages of Dorset and Norse archeological sites (e.g. Haye et al., 2005; Jensen, 2005). However, more recent work (Appelt and Gulløv, 2009; Sutherland, 2009) has presented evidence of Norse-Dorset interaction.

Terrestrial (telluric) iron is known to occur widely but invariably in very small amounts with the exception of substantial deposits in the igneous rocks of Disko Island, western Greenland. The Miocene basalts of Disko Islands have been described in detail by Clarke and Pedersen (1976) who cited many earlier studies. They found the host of native iron to be basaltic lavas and tuffs hundreds of meters thick in which native iron occurs together with sulfide minerals. The native iron is in the form of lenticular blobs (Nielsen, 1976), described by Buchwald

(1975) as typically pea sized. However, he also noted that kilogram-sized blobs of terrestrial iron reported by early explorers were ultimately found to have come from Ovifak on the south coast of Disko Island, where masses totaling in excess of 35 tonnes were found.

The foregoing indicates that any of the three possible sources of iron artifacts recovered from Dorset Culture and precontact Inuit sites are candidates as the supplier of iron. Investigation of the compositional and structural features of the metal is required in order to make the correct determination.

2. Materials and methods

2.1. Materials

Fourteen samples were received from the Canadian Conservation Institute, Department of Canadian Heritage, contained in polyester resin blocks 15 mm square. The metal samples were highly polished yielding a roughly rectangular 1 × 2 mm cross-section. The source of the artifacts from which the samples were obtained is listed in Table 1. The locations of the artifact sites are shown in Fig. 2.

2.2. Methods

The high polish on the sample surfaces was suited for examination by reflected light microscopy. The surfaces were examined and photographed to select areas for subsequent energy dispersive analyses.

The samples were semi-quantitatively analyzed for nickel-content using a defocussed electron beam. Nickel was standardized with NBS809B (Table 2) on a Hitachi 570 scanning electron microscope using the Link Isis analytical system with Super ATW thin window operated at 20 kV and 0.86 nA.

The samples were quantitatively analyzed by energy-dispersive analysis utilizing the Oxford Aztec system with the Hitachi SU70 Schottky field emission scanning electron microscope. The instrument was operated with a 24 keV acceleration voltage, a beam current of 800 mA, a count time of 40 s and a spot size of 10 μm. The analyses were standardized against the hexahedrite Filomena (Table 2). The metal of hexahedrites is of uniform composition and is widely employed as a standard in the analysis of iron meteorites. The accuracy of analyses was confirmed by use of the standard steel NBS809B as an internal standard (Table 2). The Filomena calibration was 5.52 ± 0.30 wt% Ni (s.d. n = 14), and the internal standard NBS809B yielded 3.27 ± 0.19 wt% Ni (s.d. n = 11). Samples were also mapped for Ni, Fe, Cr and P using back-scattered electrons in order to ascertain the identity of kamacite and taenite and to locate very small inclusions of schreibersite.

Table 1
Source and Artifact Numbers of samples.

Site	Artifact Numbers	Sample Description
Qariaraqyuk – Somerset Island	PaJs-2:280	unidentified iron fragment
Classic precontact Inuit (“Classic Thule”)	PaJs-2:445	iron blade fragment
(Whitridge, 1992)	PaJs-2:501	complete ulu/baleen shave (iron/bone)
Arvik – Little Cornwallis Island	QjJx-1:5	iron flake
Late Dorset	QjJx-1:6	iron lump
(Helmer, 1995b)	QjJx-1:17	possible iron blade
	QjJx-1:45	iron flake
	QjJx-1:58	iron flake
	QjJx-1:60	iron fragments
	QjJx-1:63	iron fragments
	QjJx-1:65	iron flake
	QjJx-1:71	possible iron blade
Tasiarulik – Little Cornwallis Island Late Dorset (Helmer, 1995a)	QjJx-10:3852	iron flake
Dundas Island Late Dorset (McGhee, 1981)	RaJu-4:5	unidentified iron object

Fig. 2. Locations of recovery sites of the iron artifacts analyzed in this study.

Table 2
Composition of standards Data from Wasson et al. (1998).

Element	Filomena	NBS809B
As (ppm)	4.73	154
Au (ppm)	0.612	0.045
Co (wt%)	0.454	0.0247
Cr (ppm)	68	712
Cu (ppm)	134	1024
Ga (ppm)	58.6	9.7
Ge (ppm)	177	–
Ir (ppm)	3.37	0.005
Ni (wt%)	5.65	3.23
Pt (ppm)	20.7	4.1
Re (ppb)	234	–
Sb (ppb)	–	17,100
W (ppb)	256.2	1.86

Dash indicates not determined.

3. Theory

3.1. Petrographic features

The presence of three minerals, taenite (γ-Fe), schreibersite ($(Fe,Ni)_3P$) and daubréelite ($FeCr_2S_4$), occur commonly in iron meteorites (Buchwald, 1975) and at one time were believed to occur exclusively in meteorites (Neuerburg, 1946). These minerals occur rarely in terrestrial rocks under particular conditions. Taenite occurs in iron meteorites as lamellae in the Widmanstätten structure or portions of it seen in polished section. Terrestrial occurrences of taenite are found in a few cases in mafic intrusions accompanying sulfide minerals including daubréelite in the Merensky Reef of the Bushveldt Igneous Complex (Kottke-Levin et al., 2008).

The terrestrial occurrence of schreibersite differs from that of taenite in that it is associated with other phosphorus minerals in high-grade metamorphic rocks in the Negev Desert of Israel (Gross, 1977; Burg et al., 1991). The formation of these phosphide minerals may be attributed to metamorphism of phosphate-rich sedimentary rocks. However, this occurrence differs from the schreibersite in the habit of rhabdites, small, euhedral crystals. Clarke and Goldstein (1978) demonstrated that rhabdites form in iron meteorites with low initial phosphorus content by homogeneous nucleation at 600 °C, conditions not corresponding to this terrestrial occurrence.

The case of the terrestrial iron of Disko Island presents somewhat more problematical occurrences of these minerals. Pauly (1969) reported the presence of traces of schreibersite surrounding iron spherules. The presence of minor schreibersite in globular iron nodules was also mentioned by Pedersen (1981). Ulff-Møller (1990) illustrated the occurrence of steadite, a eutectoid intergrowth of schreibersite and kamacite, as small inclusions in 1–5 mm iron spherules in basalt.

These terrestrial occurrences of schreibersite can be distinguished from meteoritic schreibersite. In the first example, the schreibersite is associated with other phosphorus minerals but not with meteoritic iron. In the Disko Island occurrences, the habit differs from that seen in meteorites, in the case of rhabdites (Clarke and Goldstein, 1978).

3.2. Kamacite bandwidths

The Widmanstätten structure in iron meteorites is the result of the exsolution with declining temperature of kamacite (α-Fe) from a taenite (γ-Fe) solid solution. The structure is composed of lamellae of kamacite alternating with lamellae of residual taenite arranged parallel to the faces of an octahedron, hence octahedrite. The general lack of overall equilibrium between exsolved kamacite lamellae and taenite leads to an Ni-concentration profile across the width of a lamella, the shape of which depends on the average thickness of kamacite bands. The profile has an M-shape across the width of a lamella (Fig. 3). However, it should be noted that the profile can be predicted to flatten as equilibrium is approached. As well, the narrower the lamella, the more likely that equilibrium will be approached owing to the shorter diffusion distance. The study of the Widmanstätten structure requires a sophisticated treatment (see Appendix 1). The Widmanstätten structure, deformed by cold working, is illustrated in Fig. 4.

We analyzed the Widmanstätten pattern following the work of Goldstein (1965), specifically his Figs. 8 and 9. He first showed that Ni in kamacite correlates with the bulk Ni concentration in a meteorite. Accordingly, the Ni content of the parent meteorite can be constrained. Then he showed that the average half width of kamacite bands correlates with the average Ni content in kamacite. Accordingly, we measured the mean composition of kamacite and the widths of the kamacite bands. The applicability of Goldstein's results was tested in the case of the Cape York meteorite using its published bulk composition and its mean kamacite bandwidth (Scott et al., 1973). As shown in Fig. 5, a bulk nickel-content of 7.58 wt% Ni. corresponds to a nickel-content in kamacite of 7.10 wt% Ni. The half-width of Cape York at 0.6 mm (Scott et al. 1973) predicts a nickel-content in kamacite of 7.39 ± 0.12 (Fig. 6). Fig. 7.

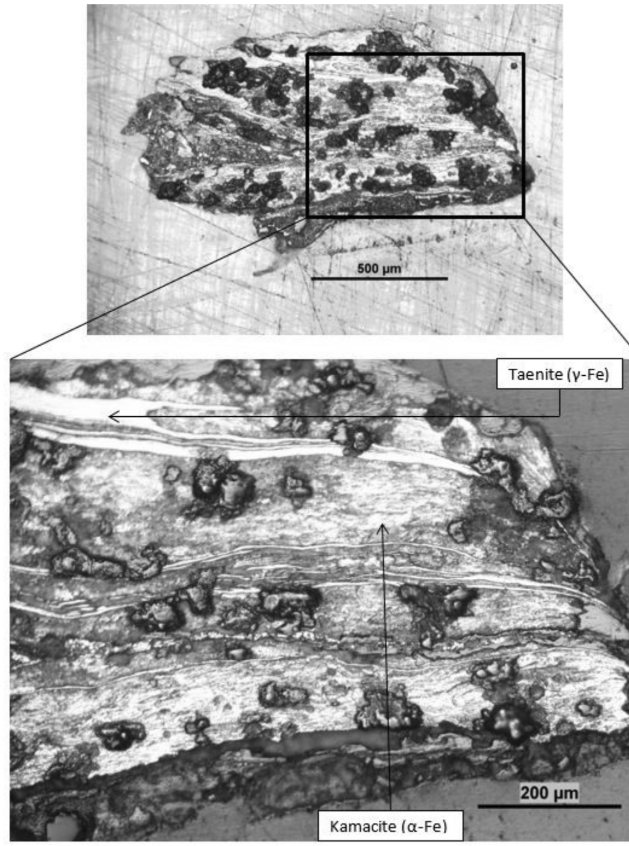

Fig. 4. Polished surface of sample PaJs-2:445 in reflected light with inset showing region analyzed. Note the abundant inclusions of oxidized metal (dark).

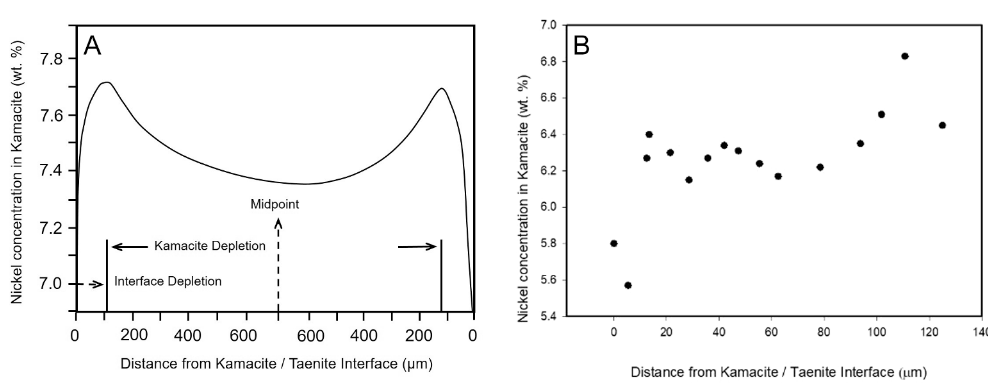

Fig. 3. (A) The M-shaped profile of nickel-content for a typical kamacite lamella. After Goldstein (1965). Used with permission of John Wiley & Sons. (B) Scan across the kamacite lamella of QjJx-1:60.

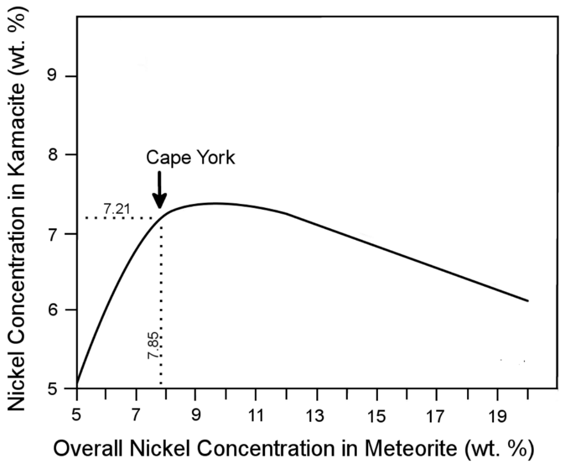

Fig. 5. The experimental relationship between bulk nickel-content of iron meteorites and mean nickel-content of kamacite. Modified after Goldstein (1965). Used with permission of John Wiley & Sons.

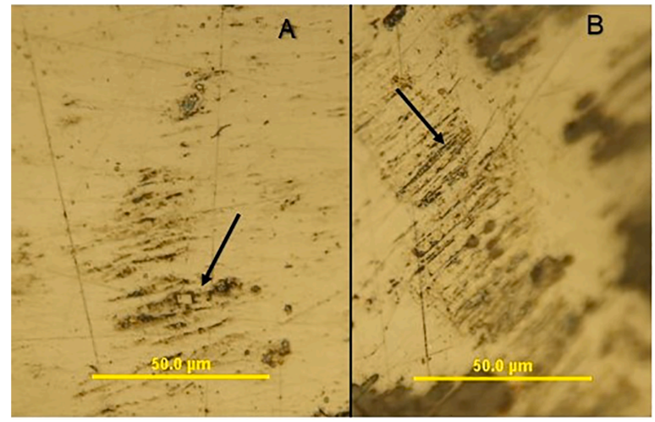

Fig. 7. A) Rhabdite in troilite nodule in reflected light (QjJx-1:71). B) Lamellae of daubréelite in troilite in reflected light (PaJs-2:280).

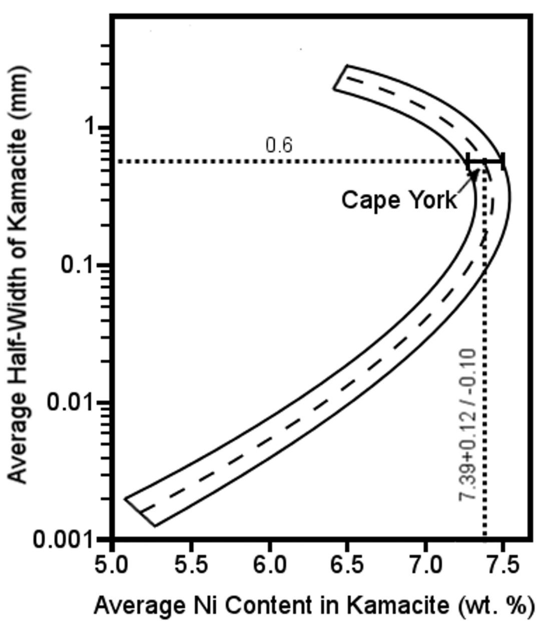

Fig. 6. The experimental relationship between kamacite bandwidth and nickel-content of kamacite. Data from literature values for Cape York are plotted. Modified after Goldstein (1965). Used with permission of John Wiley & Sons.

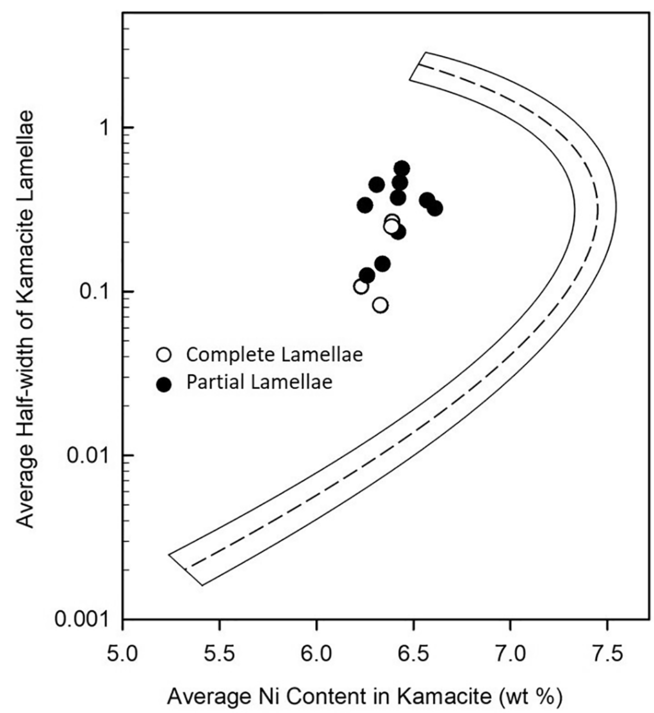

Fig. 8. Data from Table 4 plotted in relation to Goldstein's (1965) curve relating kamacite composition to half-width of lamellae.

4. Results

4.1. Petrographic examinations

Examination of the specimens by reflected light microscopy revealed various forms of evidence for their meteoritic origin as summarized in Table 3.

In the specimens of this study, well preserved rhabdites (Fig. 8A) are present in all but five cases, and their former presence in these may be inferred by holes in the iron matrix remaining after they had been weathered out. Massive schreibersite, as defined by Clarke and Goldstein (1978), is present in PaJs-2:245, QjJx-1:16, and QjJx-1:17.

Although the presence of schreibersite in most of the specimens in this study is convincing as to the meteoritic origin of the specimens in which it occurs, the presence of daubréelite, with only one terrestrial occurrence, can be considered to be diagnostic. Lamellae of daubréelite in troilite nodules were observed in PaJs-2:280 (Fig. 8B) and

QjJs-1:71. This type of occurrence was illustrated by Buchwald (1975, Fig. 530) in the Savik I mass of Cape York.

Finally, the bulk nickel composition of the specimens can be taken as evidence of the meteoritic origin of the specimens, even in the absence of other forms of evidence. Buchwald (2001) reported that in comparison with Cape York, Norse wrought iron contains less than 0.2 wt% Ni and terrestrial iron contains 1 – 4 wt% Ni. As seen in Table 3, the specimens from this study contain 6.3 – 7.9 wt% Ni based on the semi-quantitative analyses for nickel.

In conclusion, the petrographic criteria summarized in Table 3 indicate that all 14 specimens are of meteoritic origin, minimally in one case based the nickel concentration

Table 3
Evidence for meteoritic origin of specimens.

Specimen No.	Evidence of Meteoritic Origin			
	Widmanstätten Structure ($\alpha + \gamma$ Fe)[1]	Ni content (wt %)[2]	Schreibersite[3]	Daubreelite
PaJs-2:280		6.8		X
PaJs-2:245	X	7.6	X	
PaJs-2:501		6.3	r	
QjJx-1:5	γ	7.5	r	
QjJx-1:6	γ	7.0	X + r	
QjJx-1:17	X	7.2	X + r	
QjJx-1:45	γ	6.9	r	
QjJx-1:58	X	7.0		
QjJx-1:60	γ	6.8	r	
QjJx-1:63		6.8		
QjJx-1:65	γ	6.9	r	
QjJx-1:71		7.8	r	X
QjJx-10:3852	X	7.9	r	
RaJu-4:5		6.9		

[1] γ = taenite present, not in Widmanstätten structure.
[2] Semi-quantitative analysis by defocussed electron beam.
[3] If in the form of rhabdites (r).

4.2. Compositions of kamacite lamellae

The examination of the samples, as noted in Table 4, indicates that only four of the 14 samples contained portions of the Widmanstätten structure, specifically kamacite lamellae between two residual taenite lamellae. In the remaining ten samples a single taenite lamella or none is present. In these cases, the kamacite lamella in the sample was analyzed with the assumption that at least the minimum nickel-content for a complete lamella would be obtained. The analytical results are listed in Table 4. The range of Ni-content is quite narrow, 6.23–6.61 wt%, and according to the standard deviation for each sample, not significantly different at the 2σ level.

A plot of the data from Table 4 is illustrated in Fig. 8. The 14 samples appear as a cluster; however, except for the four samples containing complete kamacite lamellae (open circles), the remaining ten samples have bandwidths of undetermined size and hence would lie above their plotted positions. If the Ni-contents of the ten samples were projected upward to intersect with curve in Fig. 8, half-widths in the range 1 to 2 mm corresponding to bandwidths of 2 to 4 mm would result. This is remotely possible but very unlikely.

The distribution of nickel-content in the scan profiles was essentially flat. For all narrow lamellae scanned; the flatness of the profile may be attributable to the short diffusion distance involved. In the remaining cases, the flatness of the profile may be attributed to the location of the scan in the low-nickel center of a M-profile or to the absence of variations. The mean kamacite compositions, average 6.38 (±0.13) reported in Table 4, differs from the inferred mean composition of 7.39 wt% Ni based on the half-width measured by Scott et al. (1973). Our measured bandwidths for the complete lamellae are much narrower than the 1.2 mm reported for Savik I.

Table 4
Step-scan analysis across the kamacite bandwidths.

Sample	Mean Ni Wt % in Kamacite bw (mm)
PaJs-2:280	6.61 ± 0.24 (S.D., n = 16) > 0.321
PaJs-2:445	6.23 ± 0.66 (S.D., n = 10) 0.213*
PaJs-2:501	6.34 ± 0.19 (S.D., n = 28) > 0.147
QjJx-1:5	6.44 ± 0.18 (S.D., n = 27) > 0.333
QjJx-1:6	6.42 ± 0.24 (S.D., n = 26) > 0.231
QjJx-1:17	6.41 ± 0.58 (S.D.h, n = 33) 0.493*
QjJx-1:45	6.33 ± 0.32 (S.D., n = 26) > 0.163
QjJx-1:58	6.41 ± 0.31 (S.D., n = 14) 0.111*
QjJx-1:60	6.26 ± 0.28 (S.D., n = 21) > 0.125
QjJx-1:63	6.42 ± 0.11 (S.D., n = 13) > 0.372
QjJx-1:65A	6.57 ± 0.30 (S.D., n = 21) > 0.359
QjJx-1:71	6.25 ± 0.25 (S.D., n = 21) > 0.335
QjJx-10:3852A	6.39 ± 0.19 (S.D., n = 30) 0.531*
RaJu-4:5	6.31 ± 0.13 (S.D., n = 40) > 0.447

*Complete lamellae.

Table 5
Bandwidths (BW) and compositions of complete kamacite lamellae.

Sample Number	Half- BW (mm) measured	Kamacite wt%Ni measured	Kamacite wt%Ni theoretical
PaJs-2:445	0.107	6.23	7.32
QjJx-1:17	0.247	6.39	7.44
QjJx-1:58	0.056	6.43	7.09
QjJx-10:3852A	0.266	6.39	7.44

Goldstein (1965) determined that the effect of Ni diffusion in kamacite resulted in a change in the Ni-concentration profile in a lamella. For half-widths less than 0.1 mm not only does the Ni-content decrease as shown in Fig. 8, but the profile is that of an inverted U-shape. For half-widths >0.1 mm, an M-shaped profile is produced. At the transition between inverted U-shaped and M-shaped at 0.1 mm, the profile will approximately flat especially in the central portion of the lamella. On the other hand, the moderately well-developed M-profile in sample QjJx-1:60 (Fig. 3B) with half width > 0.125 mm is present.

The data points for complete lamellae plot to the left of the curve for the correlation between Ni-content vs. band half-width, valid for all iron meteorites (Table 5). The measured band half-widths (0.06–0.27 mm) are much smaller than the average half-width of 0.6 mm reported by Scott et al. (1973) for Savik I. We do not expect the kamacite composition to be altered by hammering; the same is not true for the half-width, which may be either increased or decreased. We should not be surprised that 10 of 14 samples do not exhibit complete kamacite lamellae because the sample size is too small. However, for meteorites with higher Ni bulk compositions than Savik I, the mean band half-widths are expected to be lower. For the other samples the half-width value is biased to values smaller than the average.

As a test of the application of Goldstein's (1965) method, the bandwidths of the six samples that contained complete kamacite bands bordered by taenite bands were measured. The half-widths of the kamacite bands together with the measured and theoretical nickel-contents, as determined from Fig. 8, are given in Table 5. The theoretical nickel-contents are systematically greater than the measured nickel-contents. As well, there is obviously no systematic relationship between nickel-content and bandwidth. These results may be due to the flattening of the M-profile, which would have had the effect of lowering the high nickel-content peaks on both sides of the M. The flattening observed in all six samples can be attributed to a close approach to equilibrium in the analyzed kamacite bands, which were very narrow, yielding short diffusion distances. Also, deformation of the lamellae is likely the cause of the lack of a relationship between nickel-content and bandwidth among the samples.

5. Discussion

According to the composition and mineralogy of the specimens, their meteoritic origin is beyond any doubt. It is reasonable to hypothesize that the Cape York meteorite is the source for the iron artifacts examined in this study because of its close proximity to precontact Inuit and Dorset territory. The differences in kamacite bandwidths reported in this study as compared with the mean reported by Buchwald (1975) may be attributed to two factors. First, Goldstein's (1965) plot (Fig. 8) illustrates that a wide variation in kamacite bandwidths and corresponding nickel-content of kamacite can occur in a single meteorite, as seen in the case of Canyon Diablo. The much smaller meteorites Carbo (454 kg) and Dayton (26.3 kg) were also shown to exhibit a range of kamacite bandwidths.

The well-studied Canyon Diablo meteorite has been shown to possess

Table 6
Ni-content of Cape York meteorite fragments (Esbensen et al., 1982).

Fragment	Ni(wt%)
Savik I	7.46
Savik II	7.54
Ahnighito East	7.46
Ahnighito West	7.63
Woman	7.65
Dog	7.89
Agpalilik	8.25
Thule	8.52

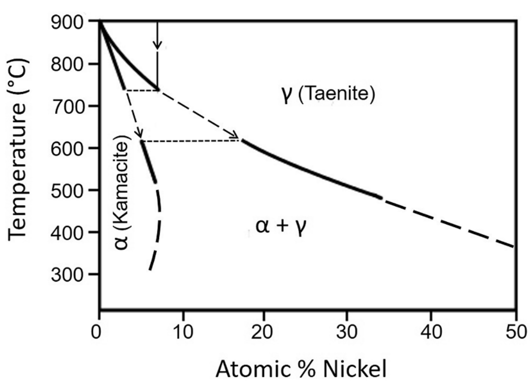

Fig. 9. High-temperature phase relations in the iron-nickel phase diagram, after Goldstein and Ogilvie (1965). The arrow shows the cooling path for a typical bulk composition leading to the formation of the Widmanstätten structure, where α is kamacite and γ is taenite. Used with permission of The Minerals, Metals & Materials Society.

a similar range of nickel-contents from 6.84 to 7.15 wt% Ni (Wasson and Ouyang, 1990). This nickel-content range corresponds to an estimated initial mass of 63,000 t (Shoemaker, 1963) based on analysis of the physics of the Canyon Diablo meteorite's crater formation. A more recent calculation gave an estimate of 300,000 to 400,000 corresponding to a spherical object 40 to 50 m in diameter (Roddy and Shoemaker, 1995). This compares with an estimate of 200 t for the initial mass of Cape York, although this is based on the assumption that the individual fragments of the Cape York meteorite are the product of a meteor shower (Buchwald, 1975). This estimated mass of the Cape York meteorite likely represents a minimum mass, as there may be undiscovered fragments.

Secondly, Buchwald's bandwidths were measured on the Savik I mass of Cape York. Esbensen et al. (1982) reported that most of the other Cape York masses were of significantly higher bulk nickel-content than Savik I (Table 6). As kamacite bandwidth in octahedrites is inversely related to bulk nickel content (e.g. Goldstein et al., 2009) in these cases, the mean kamacite bandwidths would be expected to be narrower, although they have not been reported to date.

We did expect some clarification from the study of the kamacite bandwidth concerning the exact Ni content of the meteorite. Instead it showed that the artifacts are severely deformed and the bandwidth is no longer representative of a pristine meteorite. In addition the small size of the samples is not appropriate to measure a correct value of the bandwidth in coarse meteoritic structures.

6. Conclusions

The petrographic examination together with semi-quantitative analyses of bulk composition confirms that the 14 samples from iron artifacts are of meteoritic origin. As has been demonstrated, this type of examination will identify meteoritic metal even in the absence of compositional data. Moreover, this type of procedure is applicable to any type of iron artifact where a minimal loss of material is desired.

Application of the kamacite composition technique in the effort to identify the source for meteoritic material does encounter some serious problems. As shown previously, the method seems to be viable if the mean bandwidth of kamacite lamellae are known. However, if only one or at most a few bandwidths are available in a specimen, the measured mean bandwidth is not likely to be diagnostic.

In this study, the kamacite bandwidths measured are much narrower than the mean bandwidth for the Savik I mass of Cape York Moreover, they do not lie on the theoretical curve for bandwidth vs. kamacite composition. This discrepancy can be attributed to flattening of the kamacite lamellae by cold working. Based on this method and under these circumstances, the material cannot be clearly attributed to Cape York meteorite source. However, in the case of meteoritic artifacts not subjected to intense deformation by cold working the method may offer the possibility of identifying the source meteorite.

CRediT authorship contribution statement

Matthew J.O. Svensson: Investigation, Writing - original draft, Writing - review & editing. **Stephen A. Kissin:** Writing - original draft, Writing - review & editing. **Marie-Claude Corbeil:** Conceptualization, Writing - review & editing. **Peter Whitridge:** Writing - review & editing. **James W. Helmer:** Writing - review & editing.

Declaration of Competing Interest

The authors declare that they have no known competing financial interests or personal relationships that could have appeared to influence the work reported in this paper.

Acknowledgments

We should like to thank A.D. Mackenzie for assistance with semi-quantitative analyses of the specimens and G. Wu for assistance with the quantitative scan of the samples, both of the Lakehead University Centre for Analytical Services. We thank Department of Geology technicians A. Hammond and K. Tavener for sample preparation and S.T. Spivak for drafting services.

Appendix

The basis for the method employed in this study rests on the partitioning of Ni between kamacite and taenite which varies upon cooling, as illustrated in the iron-nickel phase diagram of Goldstein and Ogilvie (1965), (Fig. 9). At high temperature, the metal exhibits the crystal structure of taenite (γ-Fe) with e.g. 7% Ni. It consists of a single phase until reaching the two phase boundary, near 750 °C, where kamacite (α-Fe) starts to exsolve forming lamellae. The compositions of the exsolved kamacite and remaining taenite at equilibrium are given by a tie-line (line at constant temperature joining the boundaries of the two phase region). As the Ni content of taenite increases with decreasing temperature, the width of kamacite lamellae increases but at the same time new lamellae may form. At equilibrium, taenite should disappear when the Ni content of kamacite equals that of the starting metal (near 500 °C for a bulk Ni content below 7%). Formation of the Widmanstätten structure is not as simple as illustrated in Fig. 9. Yang and Goldstein (2005) described in detail the mechanisms for formation of the structure, which are strongly dependent on the phosphorus-content in the Fe-Ni-P system. There have been revisions to the iron-nickel phase diagram, particularly below 400°C (Yang et al., 1996). As well, there have been more recent determinations of the diffusion coefficients for nickel in iron, and cooling rates for differing chemical groups of meteorites. However, the result of any of the mechanisms is still adequately illustrated by the Goldstein and Ogilvie (1965) phase diagram. No more recent determinations of the nickel-content in kamacite are known to us to have been made. At the level of precision in our application of Goldstein's model, differences in some of the parameters used in the diffusion calculations do not appear to have a significant effect on the applicability of the model.

The observation of meteoritic metal shows that for low-Ni meteorites (hexahedrites) the metal is homogeneous kamacite, as expected according to the phase diagram. Notice that in this case exsolution should be completed at a temperature of about 600 °C.

For meteorites with a moderate Ni concentration (6–7%, coarse to medium octahedrites) the result of the exsolution process is formation of the Widmanstätten structure, in which kamacite lamellae are oriented parallel to the faces of an octahedron separated by residual lamellae of taenite. According to the phase diagram exsolution should go to completion, but it is not the case in meteorites. In other words at some temperature the diffusion becomes too sluggish and the growth of the kamacite bands stops.

For meteorites with Ni in the range 7–16% (medium to fine octahedrites) taenite must be present even at low temperature, but the exsolution may stop before completion because of the too sluggish diffusion at low temperature. For meteorites with Ni in excess of 16% (ataxites) exsolution is expected to start atabout 630 °C. These meteorites do not exhibit the Widmanstätten pattern because of too slow diffusion.

The average composition of the kamacite lamellae are primarily a function of the bulk Ni-content of the metal (Goldstein, 1985, Fig. 8). He plotted kamacite compositions vs. bulk Ni-content for a number of iron meteorites with varied bulk Ni-contents.

The Ni-content of kamacite increases with bulk compositions from 5 to 10 wt% Ni, then slowly decreases with increasing bulk nickel-content. At low nickel content, this is in accordance with the phase diagram. At high nickel contents the kamacite bands are thin because of the slower diffusivity in high-Ni compositions and the starting of exsolution at low temperature. The correlation between Ni in kamacite and Ni in bulk meteorite (Ni > 10%) is negative indicating that kamacite composition is not equilibrated. It suggests that exsolution stops at higher temperatures for high Ni-contents corresponding to a slower diffusivity in Ni-rich compositions. In a given meteorite, large bands are those which nucleated early and therefore are more common in low-Ni meteorites (infinite size in hexahedrites) and in a given meteorite the bandwidth is variable depending on the time at which a lamella nucleated.

Accordingly, Goldstein in his Fig. 9 plotted the nickel-content of a number of kamacite bands from individual meteorites against their half-width, showing that the Ni-content of kamacite of a particular band correlates with its bandwidth. More interestingly, there is one single correlation for all meteorites independently of their bulk nickel content.

References

Appelt, M., Gulløv, H.C., 2009. Tunit, Norsemen and Inuit in Thirteenth Century northwest Greenland - Dorset between the Devil and the deep sea. In: Maschner, H., Mason, O., McGhee, R. (Eds.), The Northern World AD 900–1400. The University of Utah Press, Salt Lake City, pp. 300–320. https://doi.org/10.14430/arctic2577.

Appelt, M., Damkjar, E., Friesen, T.M., 2016. Late Dorset. In: Friesen, T.M., Mason, O. (Eds.), The Oxford Handbook of the Prehistoric Arctic. Oxford University Press, Oxford, pp. 783–805. ISBN: 978-0-87480-955-8.

Buchwald, V.F., 1975. Handbook of Iron Meteorites. University of California Press, Berkeley. ISBN: 978-0520029347.

Buchwald, V.F., 2001. Ancient Iron and Slags in Greenland. Medd. Om Grønl.: Man Soc. 26. ISBN: 978-87-635-1254-1.

Buchwald, V.F., Mosdal, G., 1985. Meteoritic Iron, Telluric Iron and Wrought iron in Greenland. Medd. Om Grønl.: Man Soc. 9. ISBN: 978-87-17-05239-4.

Burg, A., Starinsky, A., Bartov, Y., Kolodny, Y., 1991. Geology of the Hatrurim Formation ('Mottled Zone') in the Hatrurim Basin. Isr. J. Earth Sci. 40, 107–124.

Clarke, D.B., Pedersen, A.K., 1976. Tertiary volcanic province of West Greenland. In: Escher, A., Watt, W.S. (Eds.), Geology of Greenland. The Geological Survey of Greenland, Copenhagen, pp. 364–402.

Clarke Jr., R.S., Goldstein, J.I., 1978. Schreibersite growth and its influence on the metallography of coarse-structured iron meteorites. In: Smithsonian Contributions to the Earth Sciences, 21. Smithsonian Institution Press, Washington.

Corbeil, M.-C., 1996a. Determination of Nickel in Iron and Composite Artifacts (CCI No. 0,000,910). Analytical Research Laboratory Report ARS No. 3370, Part III. Canadian Conservation Institute, Department of Canadian Heritage. Unpublished report.

Corbeil, M.-C., 1996b. Determination of Nickel in Iron and Composite Artifacts (CCI No. 0,000,908). Analytical Research Laboratory Report ARS No. 3371, Part III. Canadian Conservation Institute, Department of Canadian Heritage. Unpublished report.

Esbensen, K.H., Buchwald, V.F., Malvin, D.J., Wasson, J.T., 1982. Systematic compositional variations in the Cape York iron meteorite. Geochim. Cosmochim. Acta 46, 1913–1920. https://doi.org/10.1016/0016-7037(82)90129-6.

Friesen, T.M., 2016. Pan-Arctic population movements: The early Paleo-Inuit and Thule Inuit migrations. In: Friesen, T.M., Mason, O. (Eds.), The Oxford Handbook of the Prehistoric Arctic. Oxford University Press, Oxford, pp. 673–691. ISBN: 978-0-19976695-6.

Goldstein, J.I., 1965. The formation of the kamacite phase in metallic meteorites. J. Geophys. Res. 70 (24), 6223–6232. https://doi.org/10.1029/JZ070i024p06223.

Goldstein, J.I., Ogilvie, R.E., 1965. A re-evaluation of the iron-rich portion of the Fe-Ni system. Trans. Metall. Soc. AIME 233, 283–287.

Goldstein, J.I., Scott, E.R.D., Chabot, N.L., 2009. Iron meteorites: crystallization, thermal history, parent bodies, and origin. Chem. Erde 69, 293–325. https://doi.org/10.1016/j.chemer.2009.01.002.

Gross, S., 1977. The Mineralogy of the Hatrurim Formation, Israel. Geological Survey of Israel, Bulletin no. 70, Jerusalem.

Haye, M.G., Coltrain, J.B., O'Rourke, H., 2005. Moleular archeology of the Dorset, Thule and Sadlermuit. In: Sutherland, P.D. (Ed.), Contributions to the Study of the Dorset Paleo-eskimos. (Mercury Series, Archeological Survey of Canada Paper 167) Canadian Museum of Civilization, Ottawa, pp. 11–32. ISBN: 0-660-19414-7.

Helmer, J.W., Lemoine, G.M., Hanna, D.T. 1995a. Report on Excavations at QaJx-10 (Tasiarulik), Little Cornwallis Island, Northwest Territories, 1993. Unpublished report on file, Prince of Wales Northern Heritage Centre, Yellowknife.

Helmer, J.W., Lemoine, G.M., Hanna, D.T. 1995b. Report on the 1994 Excavations at Arvik (QjJx-1), Little Cornwallis Island, Northwest Territories. Unpublished report on file, Prince of Wales Northern Heritage Centre, Yellowknife.

Jensen, J.F., 2005. Paleo-eskimo continuity and discontinuity in west Greenland. In: Sutherland, P.D. (Ed.), Contributions to the Study of the Dorset Paleo-eskimos. (Mercury Series, Archeological Survey of Canada Paper 167) Canadian Museum of Civilization, Ottawa, pp. 93–103. ISBN: 0-660-19414-7.

Kottke-Levin, J., Gauert, C., Merkle, R., 2008. Pilot study of melt inclusions in chromites of the Merensky Reef reflecting melt compositions at Karee Mine, western Bushveld Complex, South Africa. Eos Trans. AGU, 89(53), Fall Meet. Suppl., Abstract V21A-2085.

Lemoine, G., Helmer, J., Grønnow, B., 2003. Late Dorset architecture on Little Cornwallis Island, Nunavut. Études/Inuit/Studies 27, 255–280. https://doi.org/10.7202/010804ar.

McCartney, A.P., 1991. Canadian Arctic metal trade: Reflections of prehistoric to historic story networks. In: Ehrenreich, R.M. (Ed.), Metals in Society: Theory Beyond Analysis. (MASCA Research Papers in Science and Archeology, v.8, pt 2). University of Pennsylvania Museum of Archeology and Anthropology, Philadelphia, pp. 26–43.

McCartney, A.P., Kimberlin, J., 1988. The Cape York meteorite as a metal source for prehistoric Canadian Eskimos. Meteorit. 23, 288. https://doi.org/10.1111/j.1945-5100.1988.tb01289.x.

McCartney, A.P., Mack, D.J., 1973. Iron utilization by Thule Eskimos of central Canada. Am. Antiq. 38, 328–339. https://doi.org/10.2307/27972.

McGhee, R., 1981. The Dorset Occurrence in the Vicinity of Port Refuge, High Arctic Canada. (Mercury Series, Archeological Survey of Canada Paper 105) National Museums of Canada, Ottawa. ISSN: 0317-2244.

McGhee, R., 2009. When and why did the Inuit move to the eastern Arctic? In: Maschner, H., Mason, O., McGhee, R. (Eds.), The Northern World AD 900-1400. The University of Utah Press, Salt Lake City, pp. 155–163. ISBN: 978-0-87480-955-8.

McGovern, T.H., 1979. In: McCartney, A.P. (Ed.), Thule Eskimo Culture: An Anthropological Perspective. (Mercury Series, Archeological Survey of Canada Paper 88) Canadian Museum of Civilization, Ottawa. pp. 171–188, ISBN 9781772820836.

McGovern, Thomas H., 1980. Cows, harp seals, and churchbells: adaptation and extinction in Norse Greenland. Hum. Ecol. 8 (3), 245–275. https://doi.org/10.1007/BF01561026.

Maxwell, M.S., 1985. Prehistory of the Eastern Arctic. Academic Press, Orlando, FL. ISBN: 0124812708.

Nielsen, B.L., 1976. Economic minerals. In: Escher, A., Watt, W.S. (Eds.), Geology of Greenland. The Geological Survey of Greenland, Copenhagen, pp. 460–486.

Neuerburg, G.J., 1946. A preliminary note on the exclusively meteoritic minerals. Meteorit. 3, 255–258.

Park, R., 2016. The Dorset-Thule transition. In: Friesen, T.M., Mason, O. (Eds.), The Oxford Handbook of the Prehistoric Arctic. Oxford University Press, Oxford, pp. 807–825. ISBN: 9780199766956.

Pauly, H., 1969. White cast iron with cohenite, schreibersite, and sulphides from Tertiary basalts from Disko. Greenland. Medd. Dansk Geol. Foren. København 19, 8–26.

Pedersen, A.K., 1981. Armalcolite-bearing Fe-Ti oxide assemblages in graphite-equilibrated salic volcanic rocks with native iron from Disko, central West Greenland. Contrib. Mineral. Petrol. 77 (4), 307–324. https://doi.org/10.1007/BF00371560.

Raghavan, M., and 56 others, 2014. The genetic prehistory of the New World Arctic. Science 345 (6200), 1255832–1-9. https://doi.org/10.1126/science1255832.

Roddy, D.J., Shoemaker, E.M., 1995. Meteor Crater (Barringer Meteorite Crater), Arizona: summary of impact conditions. Meteorit. 30, 567. https://doi.org/10.1111/j.1945-5100.1995.tb01298.x.

Schledermann, P., 1980. Notes on Norse finds on the east coast of Ellesmere Island, NWT. Arctic 33, 454–463. https://doi.org/10.14430/arctic2577.

Scott, Edward R.D., Wasson, John T., Buchwald, V.F., 1973. The chemical classification of iron meteorites-VII. A reinvestigation of irons with Ge concentrations between 25 and 80 ppm. Geochim. Cosmochim. Acta 37, 1957–1983. https://doi.org/10.1016/0016-7037(73)90151.

Shoemaker, E.M., 1963. In: Middlehurst, B., Kuiper, G.P. (Eds.), The Moon, Meteorites, and Comets. The Solar System, 4. University of Chicago Press, Chicago, pp. 301–336.

Sutherland, P.D., 2009. The question of contact between Dorset Paleo-Eskimos and early Europeans in the eastern Arctic in Maschner, H., Mason, O., McGhee, R. (Eds.) The Northern World AD 900-1400. The University of Utah Press, Salt Lake City, pp. 279-299. ISBN: 978-0-87480-955-8.

Ulff-Møller, Finn, 1990. Formation of native iron in sediment-contaminated magma. I. A case study of the Hanekammen Complex on Disko Island, West Greenland. Geochim. Cosmochim. Acta 54, 57–70. https://doi.org/10.1016/0016-7037(90)90195-Q.

Wasson, J.T., Choi, B.-G., Jerde, E.A., Ulff-Møller, F., 1998. Chemical classification of iron meteorites XIIl. New members of the magmatic groups. Geochim. Cosmochim. Acta 71, 715–724. https://doi.org/10.1016/S0016-7037(97)0037.

Wasson, J.T., Ouyang, X., 1990. Compositional range in the Canyon Diablo meteoroids. Geochim. Cosmochim. Acta 54, 3175–3183. https://doi.org/10.1016/0016-7037(82)90129-6.

Whitridge, P., 1992. Archaeological Investigations at Port Leopold, Somerset Island: Report of the 1991 Field Season. Unpublished report on file, Prince of Wales Northern Heritage Centre, Yellowknife.

Whitridge, P., 1999. The Construction of Social Difference in a Prehistoric Inuit Whaling Community. PhD dissertation. Arizona State University, Tempe, AZ.

Whitridge, P., 2002. Gender, households, and the material construction of social difference: Metal consumption at a Classic Thule whaling village. In: Frink, L., Shepard, R., Reinhardt, G. (Eds.), Many Faces of Gender: Roles and Relationships Through Time in Indigenous Northern Communities. University of Colorado Press, Boulder, pp. 165–192. ISBN: 1552380939.

Whitridge, P., 2016. Classic Thule [Classic Precontact Inuit]. In: Friesen, T.M., Mason, O. (Eds.), The Oxford Handbook of the Prehistoric Arctic. Oxford University Press, Oxford, pp. 827–849. ISBN: 9780199766956.

Wright, J.V., 1995. A History of the Native People of Canada, v.1. (Mercury Series, Archeological Survey of Canada Paper 152). Canadian Museum of Civilization, Hull, QU. ISBN: 0660159511.

Yang, C.W., Goldstein, J.I., 2005. The formation of the Widmanstätten structure in meteorites. Meteorit. Planet. Sci. 40, 239–253. https://doi.org/10.1111/j.1945-5100.2005.tb00378.x.

Yang, C.W., Williams, D.B., Goldstein, J.I., 1996. A revision of the Fe-Ni phase diagram at low temperature. J. Phase Equilib. 17, 522–531. https://doi.org/10.1007/BF02665999.